JOURNAL OF GEOPHYSICAL RESEARCH, VOL. 91, NO. C6, PAGES 7680–7690, JUNE 15, 1986

CTD and Velocity Surveys of Seaward Jets Off Northern California, July 1981 and 1982

P. MICHAEL KOSRO AND ADRIANA HUYER

College of Oceanography, Oregon State University, Corvallis

Two mesoscale surveys were conducted (in July 1981 and July 1982) near Point Arena, California, to determine the structure and circulation associated with tongues of cold surface water extending seaward from the coastal zone. Both surveys were designed at sea on the basis of available satellite IR data, and each was completed in less than a week. Sampling extended 100 km alongshore and 150 km (1981) to 250 km (1982) offshore, and included conductivity, temperature, and depth casts to 500 dbar, and continuous ocean current profiling to 150 m by means of a Doppler acoustic log. Both surveys showed that the tongues of cold water seen in the satellite images were the surface manifestation of hydrographic and current anomalies that extended to a depth of at least 100 m. In each case, strong seaward flow was observed along the northern edge of the cold tongue, which also marked a shallow water mass boundary between low-salinity (< 32.8 ppt) surface waters to the north and high-salinity (> 33.2 ppt) waters to the south. The seaward jets were very strong (up to 80 cm/s) and narrow (30 km), with strong shears (up to 10^{-2} s^{-1} in the vertical and up to 10^{-4} s^{-1} in the horizontal). They were largely geostrophic, had transports exceeding 1.5 sverdrups, and can persist for 2–3 weeks. The seaward jets seemed to be continuous with southward flowing alongshore coastal jets. There is evidence that the seaward jets are recurrent features in the vicinity of Point Arena.

INTRODUCTION

Prominent tongues or plumes of cold water, some measuring hundreds of kilometers in length, have long been recognized in satellite infrared images of sea surface temperature off the California coast [*Bernstein et al.*, 1972] (see Figure 1). The surface manifestations of these features have been analyzed from satellite data [*Breaker and Gilliland*, 1981; *Kelly*, 1985; *Ikeda and Emery*, 1984]; however, prior to 1981, in situ measurements of the temperature field had been obtained only rarely [*Bernstein et al.*, 1972; *Traganza et al.*, 1981], and none had been made of the salinity or current fields. In July 1981, guided by satellite imagery, we conducted a shipboard survey to determine the structure and circulation associated with one such cold tongue off northern California, seaward of the Coastal Ocean Dynamics Experiment (CODE) region. A second cold tongue in the same area was surveyed during July 1982.

In this paper, we will present the results of those surveys. We will describe the mesoscale structure of the observed temperature, salinity, density, and current fields; relate the observed features to those seen in the satellite images; and relate the directly measured (Doppler acoustic log, or DAL) currents to the distributions of water properties and to estimates of the geostrophic flow. Finally, we shall discuss the relationship of the observed seaward jets to the southward surface current flowing along the Oregon and northern California coast in summer.

THE OBSERVATIONS

The surveys were made as part of CODE [*CODE Group*, 1983]. The data included hydrographic casts at discrete locations and continuous ocean current profiling by means of a DAL.

Paper number 6C0020.
0148-0227/86/006C-0020$05.00

The hydrographic observations were made with a Neil Brown Mark III-B conductivity, temperature, and depth (CTD) system, using a lowering rate of about 45 m/min, to a maximum depth of 500 m, or to within 5–20 m of the bottom over the continental shelf and upper slope. CTD data processing included correcting the conductivity data to agree with in situ calibration samples, filtering to allow for differences in sensor response times, and averaging the calculated salinity and temperature data into 1- or 2-dbar bins [*Gilbert et al.*, 1981]. Accuracy of the final processed pressure, temperature, and salinity data is believed to be ±2 dbar, ±0.01°C, and ±0.003 ppt, respectively. At each CTD station, we also recorded wind speed and direction. The CTD data from these surveys have been summarized in data reports by *Olivera et al.* [1982] and *Huyer et al.* [1984].

Current profiling was performed continuously along the ship's track using an Ametek-Straza DAL. The data processing techniques, an error analysis, and comparison with moored current meters are fully described by *Kosro* [1985]. Current profiles typically spanned the depth range 15–150 m, with measurements separated vertically by 6.5 m. Estimates of the currents were obtained by filtering the combined DAL and navigation (LORAN-C) data over 30 min. Comparison of shipboard current measurements processed in this way with those from vector measuring current meters moored over the shelf and slope during CODE showed differences with standard deviations of 5 cm/s; correlations between the shipboard and moored measurements were 0.95–0.97 for the energetic alongshore component of the currents, 0.76–0.82 for the much weaker cross-shore component.

The sampling patterns (Figure 2) in the offshore waters were designed at sea on the basis of available sea surface temperature (SST) information: in 1981, we had facsimile SST maps transmitted from Redwood City by the National Weather Service as well as precruise satellite infrared images provided by K. Kelly; in 1982, L. Armi transmitted copies of satellite infrared images directly to the ship. The goal was to sample within and across the surface temperature front or cold filament seen

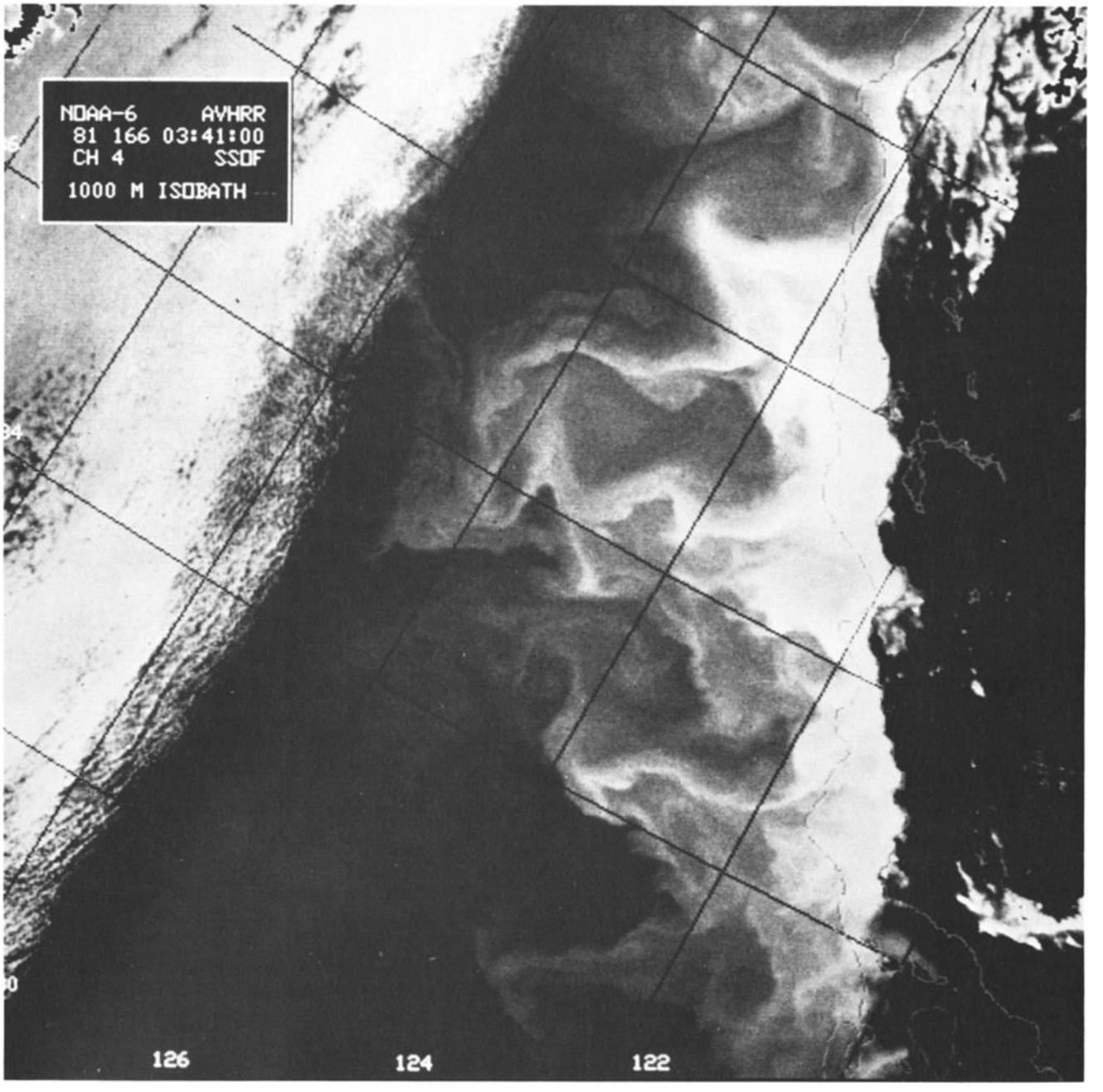

Fig. 1. Satellite (NOAA 6) infrared image of sea surface temperature on June 15, 1981, showing at least four large tongues of cold water between Cape Mendocino and Point Conception (image provided by Pierre Flament).

in the satellite images. Each survey also included sampling of the coastal waters over the continental shelf. During both surveys, upwelling favorable winds increased from only a few knots during the first day or so to sustained levels of 15–30 knots.

The first survey (Figure 2) was completed in just under 5 days, from 1950 UT on July 4 to 1500 UT on July 9, 1981. Satellite images from July 6, 7, and 8 [*Kelly*, 1982] showed little change in the surface temperature field, suggesting that the survey was at least quasi-synoptic (however, the field had evolved substantially since June 28, the date of the precruise image used to design the sampling pattern). Samples were obtained across the front separating the cold tongue from the warm waters to the north.

Our second survey was conducted the following year, from 1840 UT on July 19 to 0646 UT on July 26, 1982. L. Armi, P. Flament, and L. Washburn of Scripps Institution of Oceanography participated in the 1982 cruise in order to make "tow-yo" CTD observations through the small-scale, presumably dissipative, eddies observed along the edges of the cold tongues [*Flament et al.*, 1985]. This group also provided an underway system to monitor surface temperature and salinity, and ship-to-shore communications that enabled us to receive copies of satellite images at sea. The 1982 survey extended much farther out to sea (250 versus 150 km) than the 1981 survey (Figure 2). The typical CTD station spacing in the offshore region was much coarser ($\simeq$30 km) in 1982 than it had been ($\simeq$10 km) in 1981, but the underway sampling

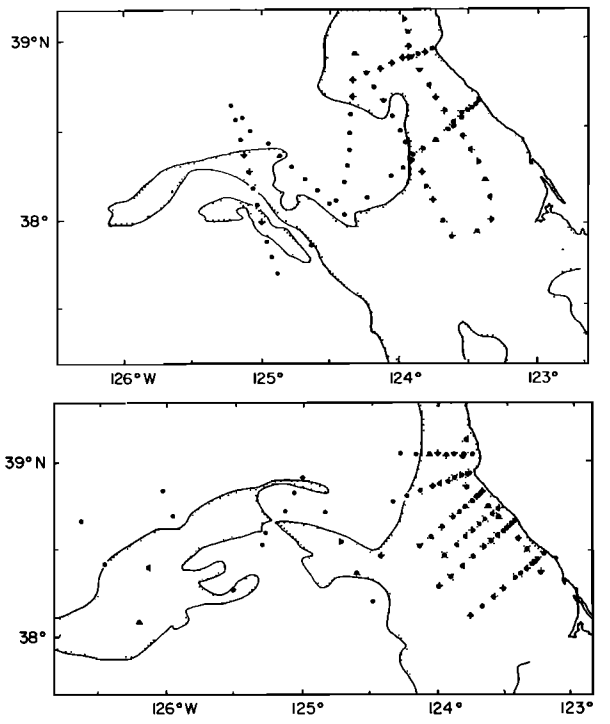

Fig. 2. CTD station positions during the two CODE surveys of cold tongues near Point Arena conducted during (top) July 4–9, 1981, and (bottom) July 19–26, 1982. Shaded area indicates relatively cold areas seen in satellite IR images.

system allowed us to resolve very small-scale features in the surface layer in real time. Although the full survey took almost a week to complete, the 15 offshore CTD stations, representing five crossings of the cold filament, were obtained in less than 36 hours on July 24 and 25.

RESULTS

Surface Fields and Currents

Satellite images from July 8, 1981, and July 22, 1982, are presented in Figure 3. In 1981 a narrow (~10 km wide), convoluted filament of cold water extends 250 km seaward from its apparent point of origin in the coastal region. Seaward of 125°W, this coldest filament marks the perimeter of a much broader (~100 km wide) cool tongue, also rooted in the coastal region. A pool of warm water borders the cool tongue in the north, at its point of departure from the coastal zone. The morphology of the cold tongue surveyed in 1982 is strikingly similar.

The directly measured current vectors from 28-m depth have been superimposed on each image (Figure 3). These measurements reveal that the thermal features seen at the surface in the satellite images (tongues or plumes) are associated with strong seaward current features (jets or squirts) reminiscent of those observed over the continental shelf and slope [*Davis*, 1985*a*; *Kosro*, 1985]. The largest component of the current is generally directed along the temperature fronts, the currents veering anticyclonically from downcoast to seaward around the southern edge of a warm water pool south of Point Arena. In both years, maximum seaward currents exceeded 80 cm/s. In 1981, in the southwest corner of the survey, a zone of return flow was observed, with currents directed back toward the coast at 40 cm/s. A similar return flow during 1982 has been inferred from sequences of satellite images [*Flament et al.*, 1985], although the ship did not sample far enough south to directly observe it. Questions about the detailed relationship between the thermal and current fields (e.g., does the current maximum occur at the cold filament?) are best answered by an analysis of the in situ data presented below, since the satellite measurements of SST are separated from the current measurements by 28 m in depth and tens of hours in time.

The near-surface CTD measurements for 1981 (Figure 4) verify the broad thermal features seen in the July 8 satellite image: the warm pool ($T > 15$°C) bounds both the cold coastal water ($T < 10$°C) and the cool tongue ($T \simeq 13$°C) and is separated from them by a temperature front along the 14°C isotherm. This temperature front is also a strong salinity front; near-surface waters in the warm pool are uniformly fresh ($S \simeq 32.6$ ppt), while waters in the cold tongue are salty (maximum $S \simeq 33.2$ ppt) and coastal waters even more so ($S > 33.4$ ppt). Across the northern edge of the cold tongue, a very strong density front results (σ_t changes by as much as 1.2 in 10 km). These fronts along the edge of the cold tongue are continuous with the upwelling fronts in T and S that parallel the coast further to the north. Inshore of the coastal front, salinity and density increase toward the coast, as expected in an upwelling region.

In 1982, combined CTD and underway measurements of surface properties (Figure 4) again show the presence of strong gradients between a warm ($T \simeq 15$°C), fresh ($S \simeq 32.8$ ppt) pool to the north and a cooler, more saline tongue. The TS characteristics of these surface water masses are quite distinct [*Flament et al.*, 1985, Figures 12 and 13]. The 1982 survey resolves the presence of a quite narrow cold filament along the northern edge of the tongue. The axis of this filament lies along the very strong salinity front separating the cool tongue from the warm pool to the north.

Vertical Structure

The surface temperature and salinity fronts penetrate to depths of at least 30 m, and the general structure of the temperature and salinity fields penetrates to at least 100 m. This may be seen in maps of each quantity (see data reports by *Olivera et al.* [1982] and *Huyer et al.* [1984]) or in the correlations between surface and subsurface fields (Table 1). In 1981 the correlation is very high ($\simeq 0.9$) at 30 m, and the offshore anomalies in temperature, salinity, and density are at least as large as their surface values (regression coefficients consistently larger than the correlation coefficients). At 100 m, the correlation is still high (0.6–0.8), but the strength of the deeper offshore anomalies is much reduced relative to the near-surface values (regression coefficients smaller than the correlation coefficients). The results are similar for 1982, except that the salinity and density anomalies remain strong down to 100 m.

Data from two crossings of the cold tongue and associated seaward jet are shown in the vertical sections of Figure 5. For 1981 the crossing farthest from shore is shown; for 1982 the section with the densest CTD sampling is used. Because the section in 1982 crossed the jet obliquely, the measurements have been projected onto a section perpendicular to the direction of integrated transport. Current sections have been contoured from averages over bins 5 km wide.

The top panel shows the available measurements of near-surface fields for each section. For 1981, T, S, and σ_t from 5 m

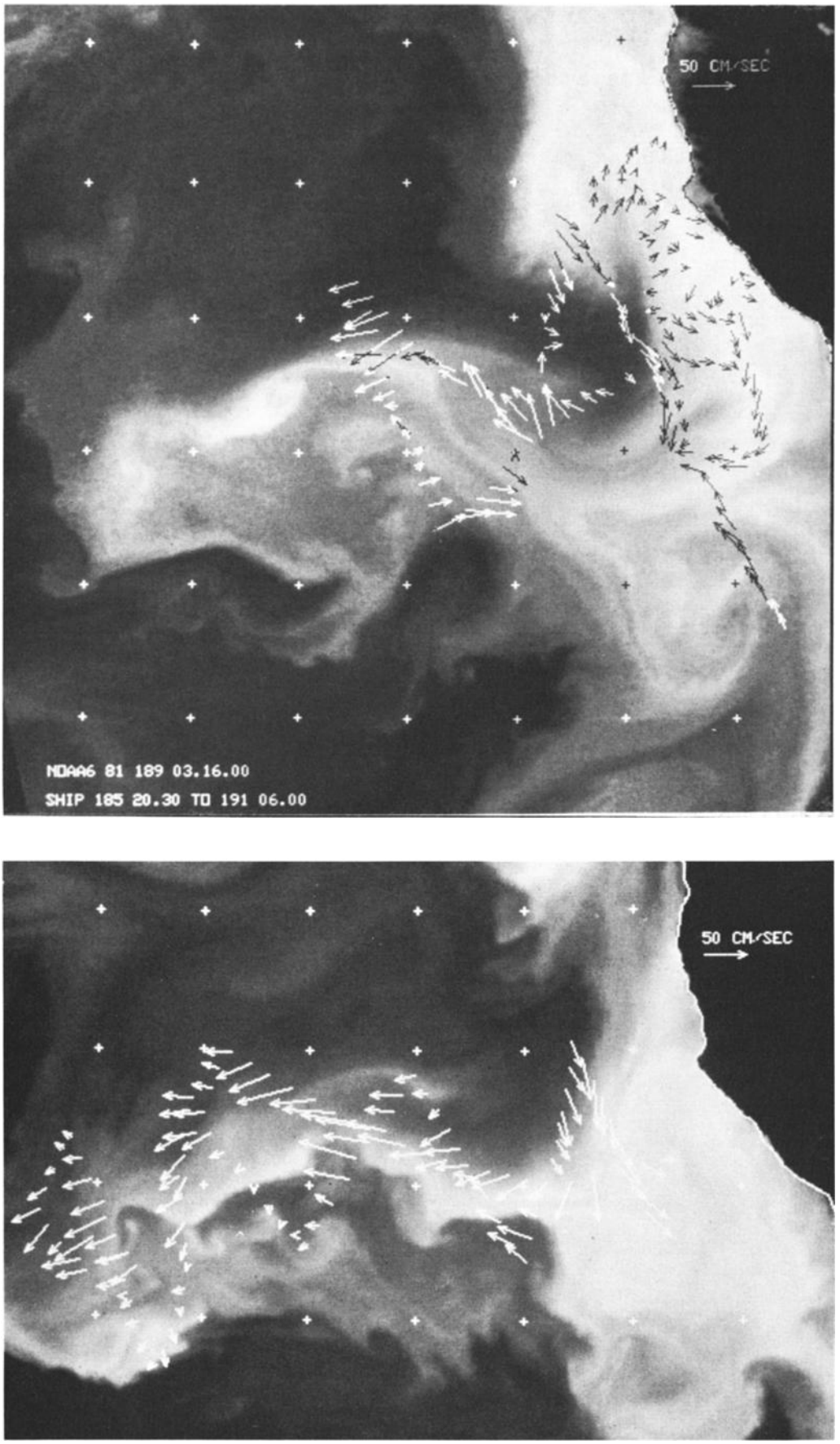

Fig. 3. DAL current vectors at a depth of 28 m from the surveys of (top) July 4–9, 1981, and (bottom) July 19–26, 1982, superimposed on the NOAA 6 infrared images of July 8, 1981, and July 22, 1982, respectively. Tics are at whole and half degrees of latitude and longitude.

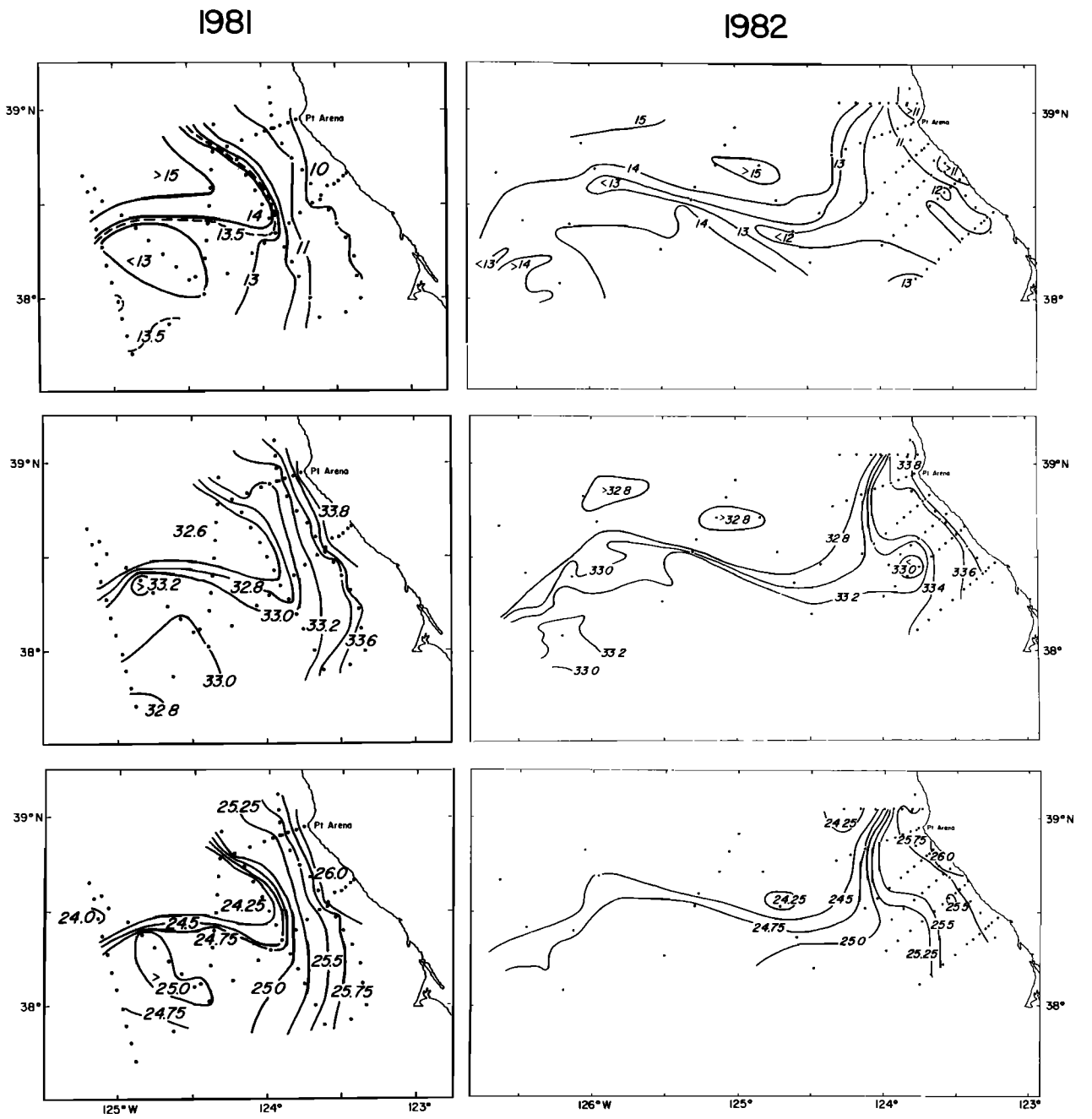

Fig. 4. Maps of the near-surface (5 m) CTD temperature, salinity, and density during the (left) July 1981 and (right) July 1982 surveys.

at each CTD station and the temperature at the ship-mounted acoustic transducer are shown. Although these latter data are known to be highly filtered representations of the actual sea surface temperature [*Kosro*, 1985], the location of the surface temperature front can be clearly seen. Just south of the front, a weak temperature minimum indicates the presence of a cold filament less than 20 km in width. At the resolution provided by the CTD station spacing, the surface temperature front coincides with a front in salinity and in density. For 1982 the underway thermosalinograph data show in detail a surface temperature minimum about 10 km wide that corresponds to the cold filament seen in the satellite images. This filament has a very sharp southern boundary that coincides with a sharp, density-compensating drop in salinity. The temperature increases gradually to the north, while the salinity remains low, leading to a gradual decrease in surface density of about the same size as seen in 1981.

In both years, the current sections show a strong, surface-intensified, baroclinic seaward jet, with core speeds up to 80 cm/s. The coldest surface water in the cold filament occurs near the strongest seaward flow; however, the width of the jet, about 30 km, is greater than the width of the cold filament. Vertical shear is high (as high as 0.03 s^{-1} near the surface in 1981, though more typically 0.005–0.01 s^{-1}) within and much lower outside this 30-km-wide zone. The horizontal shear is highly asymmetric in the 1982 section: cyclonic current gradi-

TABLE 1. Comparison of Subsurface (30 and 100 m) Fields With the Near-Surface (5 m) Fields

	Offshore Stations Only			Entire Survey		
	r	α	N	r	α	N
		1981				
T (30 m)	0.86	1.07	39	0.89	0.88	84
S (30 m)	0.88	1.02	39	0.93	0.95	84
σ_t (30 m)	0.91	1.06	39	0.93	0.92	84
$D_{z/100}$ (30 m)	0.99	0.69	39	0.99	0.65	84
$D_{z/500}$ (30 m)	0.99	0.82	35	0.98	0.81	56
		1982				
T (30 m)	0.82	1.17	17	0.88	1.13	62
S (30 m)	0.94	1.05	17	0.94	1.03	62
σ_t (30 m)	0.91	1.28	17	0.94	1.11	62
$D_{z/100}$ (30 m)	0.99	0.77	17	0.996	0.69	62
$D_{z/500}$ (30 m)	0.99	0.89	17	0.98	0.81	45
		1981				
T (100 m)	0.60	0.29	39	0.68	0.26	84
S (100 m)	0.74	0.62	39	0.76	0.46	84
σ_t (100 m)	0.80	0.48	39	0.79	0.35	84
$D_{z/500}$ (100 m)	0.78	0.34	35	0.78	0.35	56
		1982				
T (100 m)	0.51	0.40	17	0.77	0.36	62
S (100 m)	0.69	1.03	17	0.79	0.68	62
σ_t (100 m)	0.84	1.00	17	0.86	0.55	62
$D_{z/500}$ (100 m)	0.98	0.51	17	0.92	0.37	45

The correlation coefficient r, linear regression coefficient α (computed in the sense $T_{deep} = \alpha T_5 + \beta$), and number of station pairs N for each field are given. Stations located at least 25 km seaward of the 2000-m isobath have been designated "offshore" and analyzed separately.

ents of the order of $f = 10^{-4}$ s^{-1} occur at the southern boundary of the jet, at the density-compensated fronts in T and S, while anticyclonic shears are of order $f/3$ or less. This asymmetry is observed on the other crossings from 1982 [see *Kosro*, 1985] but is not evident in 1981. In 1982, currents were seaward everywhere in the study region to depths exceeding 100 m; in 1981, shoreward flow up to 40 cm/s strong was seen south of the seaward jet, the currents reversing some 40–50 km south of the maximum seaward flow.

The surface temperature and salinity data (top panels of Figure 5) indicate that surface waters to the right (i.e., north) of the jet have different TS characteristics than those to the left (i.e., south) of the jet. The depth extent of this water mass boundary can be seen in the bottom panels of Figure 5, which show salinity as a function of density. In such a presentation, a change in TS characteristics is indicated where the isohalines depart from the horizontal. In 1981 the water mass boundary extends down to the 25.5 isopycnal, i.e., to 100 m or less; in 1982 it extends deeper into the water column, to $\sigma_t \simeq 25.8$ or depths of 150 m. The core of the jet lies at, or perhaps slightly north of, this shallow water mass boundary.

Geostrophy

In both surveys the observed current vectors closely followed contours of the dynamic height field (Figure 6). For a simple quantitative comparison between geostrophic and measured currents, we calculated, for each pair of consecutive CTD stations beyond the 500-m isobath, both the average across-section component of the DAL current and the interstation estimate of geostrophic current relative to 500 dbar. In 1981 the correlation coefficient between these two estimates was 0.80 at 30 m and 0.73 at 100 m (45 pairs of current measurements); the correlation coefficient of the 30- to 100-m geostrophic shear with the across-section component of the measured shear was 0.70 for 67 pairs of stations beyond the 100-m isobath. In 1982 the correlation coefficients were 0.86 and 0.81 for the currents at 30 and 100 m (31 pairs of stations beyond the 500-m isobath) and 0.87 for the 30- to 100-m shear (44 pairs of stations beyond the 100-m isobath).

Submesoscale variability in the current and hydrographic fields (e.g., internal and intertial waves) and noise in the measurements act to reduce the correlations in the above analysis, particularly when, as in 1981, the stations are closely spaced. It is thus desirable to separate the mesoscale flow, which we expect to be largely geostrophic, from the smaller scale and more rapidly fluctuating components. Using objective analysis, we estimated the geostrophic current at the locations (see Figure 6) of all DAL current vectors beyond the 500-m isobath, and then spatially smoothed both sets of vectors with a Gaussian filter $G(r) = A \exp(-r^2/R^2)$ at a variety of smoothing lengths R [*Regier*, 1982]. The results for $R = 20$ km (Figure 7) show that, once small scales have been removed, the correspondence between measured and geostrophic currents and shears is striking. Vector correlation between the smoothed fields is 0.89, 0.87, and 0.81 (1981) and 0.88, 0.78, and 0.90 (1982) for the 30 m, 100-m currents, and 30- to 100-m shear, respectively.

The Importance of Salinity Gradients

During both surveys, maximum currents coincided roughly with a surface salinity front (cf. Figures 4 and 6) and an associated water mass boundary (Figures 4 and 5) over the entire survey region. During July 1981 the low-salinity waters to the right of the jet were warm, while the high-salinity waters to the left of the jet were cold. Within our resolution, the temperature front coincided with the salinity front, and horizontal gradients in surface temperature, salinity, and density were all correlated with the geostrophic shear in the upper layers (Table 2). Thus interpreting the satellite image of surface temperature as if it were representative of the surface density field to infer the near-surface geostrophic shear (from the thermal wind equation) would be qualitatively correct for July 1981. This applies also, though to a lesser extent, to the waters within 75 km of the coast during July 1982 (Table 2). However, in the offshore region in July 1982, the sharp salinity front coincided with a density-compensating temperature front, and the narrow temperature minimum lay within the core of the seaward jet (Figures 4 and 5), as if it were being advected offshore by the jet; there was no significant correlation between the surface temperature gradients offshore and the geostrophic shear (Table 2). Thus interpreting the July 1982 satellite image as a proxy for the near-surface density field would have been misleading.

In both years the seaward jet lay along a roughly zonal (east-west) salinity front. In part, this zonal front appears to be the result of an offshore meander in the upwelling front near Point Arena. An additional source for zonal salinity fronts may be local intensification of the large-scale mean surface salinity field, which has a definite north-south gradient in the California Current region (Figure 8). Outflow from the Columbia River and local runoff from British Columbia, Washington, and Oregon certainly contribute to this mean north-south gradient; a simple calculation shows that the

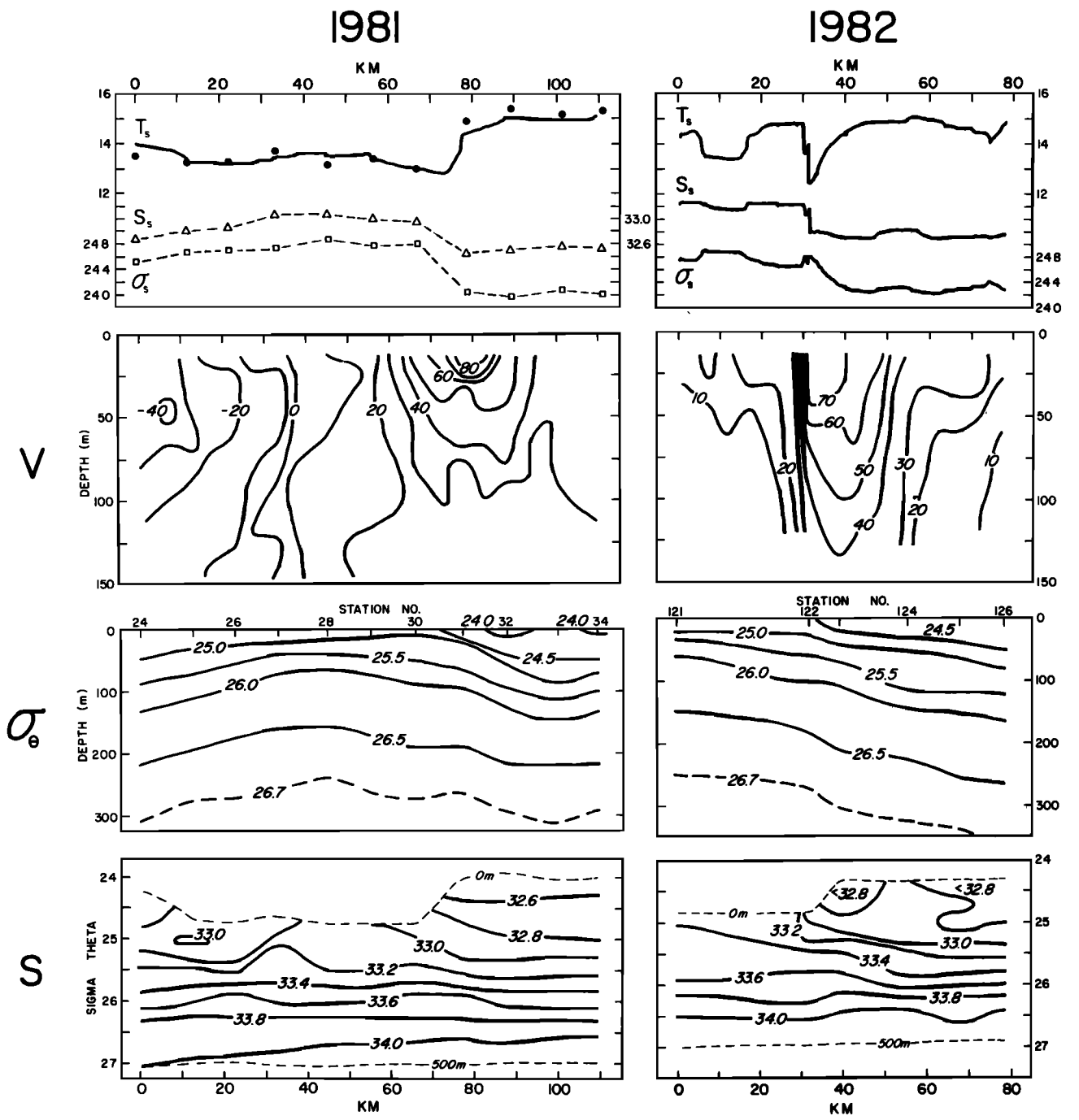

Fig. 5. Cross sections through the seaward jet centered (left) at about 38.2°N, 125.0°W in 1982 and (right) at about 38.5°N, 125.2°W in 1982. Distance axis increases to the north. Top panels show near-surface (5 m) temperature, salinity, and density (from DAL and CTD in 1981 and underway system in 1982). Middle panels show the vertical distribution of the normal component of the DAL velocity and of the density anomaly σ_θ. Bottom panels show salinity as a function of density.

average yearly Columbia River outflow of 2.5×10^{11} m^3 [*Huyer*, 1983] is sufficient to lower the salinity of the upper ocean by 0.7 ppt over a region 1500 km long, 250 km wide, and 30 m deep. These sources may also contribute to the presence of locally strong fronts, as the fresh effluent and runoff are advected south along the coast. The shallow water mass boundary observed in both 1981 and 1982 is consistent with *Olivera*'s [1983] suggestion that the jets occur along the edges of dilute remnants of the Columbia River plume.

Time Scales

Between July 31 and August 5, 1982, the OPTOMA program independently conducted an expendable bathythermograph (XBT)/CTD survey between 37.8°N, 38.7°N, 125°W, and 127°W [*Rienecker et al.*, 1985]. Their survey region overlapped with the offshore end of ours and extended somewhat farther out to sea. They too observed the narrow filament of cold surface water separating lower surface salinities (≃32.7 ppt) to the north from higher surface salinities (≃33.0 ppt) to

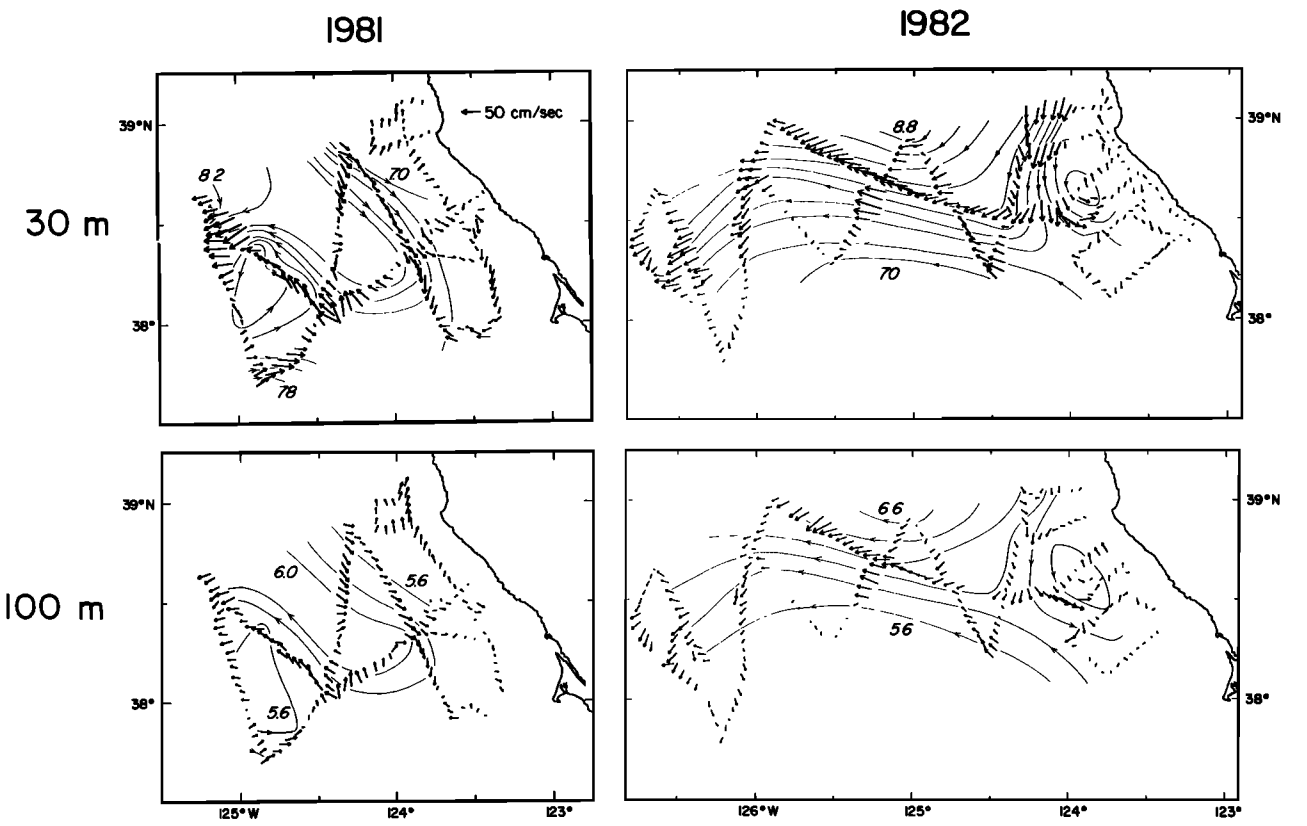

Fig. 6. Maps of the DAL current vectors at 30 and 100 m superimposed on the dynamic topography relative to 500 dbar, during the (left) July 1981 and (right) July 1982 surveys. The scale for the DAL vectors is shown in the top panel; the contour interval for the geopotential anomaly is 0.2 $m^2 s^{-2}$.

the south. They too observed in the dynamic topography a seaward jet that lay along the axis of the temperature minimum. The combination of our observations and theirs indicates that the seaward jets and the associated cold tongues can persist for at least 2 weeks.

Kelly [1985] performed an empirical orthogonal function (EOF) decomposition of the CODE 1 satellite SST images for the period April–July 1981 to determine the dominant patterns of spatial variability. The third EOF (at negative amplitudes) showed tongues of cold water extending seaward at or

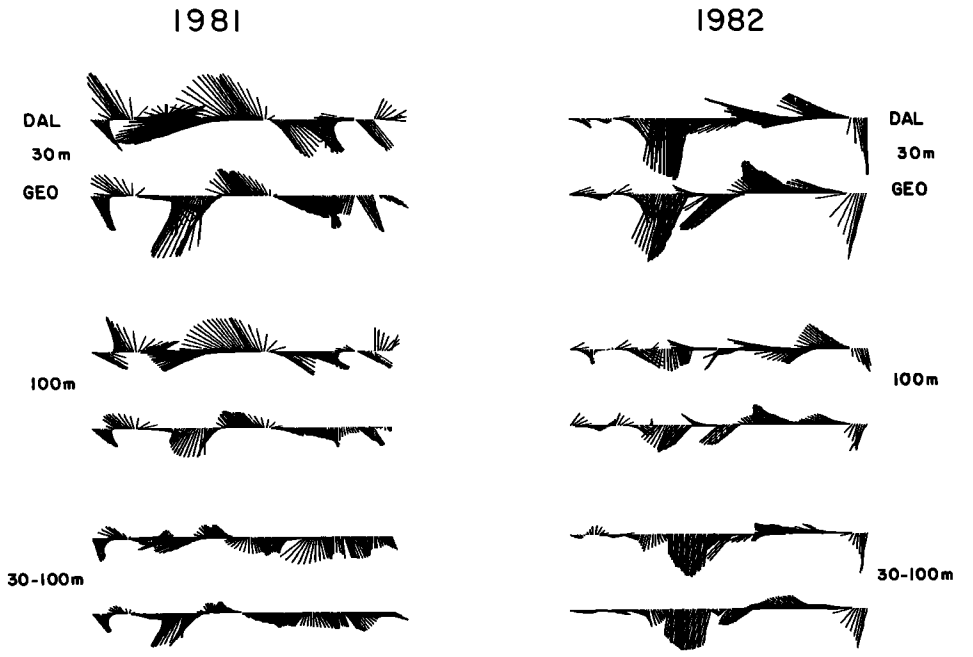

Fig. 7. Comparison of DAL velocity vectors to geostrophic velocity vectors obtained from an objective analysis of the CTD data. Both DAL and geostrophic velocities have been smoothed with a smoothing length of 20 km. Each panel shows successive DAL vectors along the ship's track and the corresponding geostrophic velocity vectors. (Obvious discontinuities are due to gaps in the DAL data.)

TABLE 2. Correlation of the Dynamic Height Difference Between Station Pairs With Near-Surface (5 m) Difference in Temperature, Salinity, and Density

		ΔT_5	ΔS_5	$\Delta\sigma_5$	N
Offshore					
1981	$\Delta D_{5/100}$	0.68	−0.57	−0.68	30
	$\Delta D_{30/100}$	0.50	−0.41	−0.49	30
1982	$\Delta D_{5/100}$	0.23	−0.62	−0.74	16
	$\Delta D_{30/100}$	0.04	−0.62	−0.57	16
Nearshore					
1981	$\Delta D_{5/100}$	0.88	−0.81	−0.92	40
	$\Delta D_{30/100}$	0.80	−0.72	−0.82	40
1982	$\Delta D_{5/100}$	0.52	−0.69	−0.69	34
	$\Delta D_{30/100}$	0.34	−0.52	−0.50	34

Separate statistics are shown for station pairs located nearshore, where flow is predominantly alongshore, and for pairs located far from shore, where flow is predominantly seaward; these regions were divided along a line 25 km (one Rossby radius) beyond the 2000-m isobath.

just north of Cape Mendocino, Point Arena, and Point Reyes, with warm water in between. The time series of its amplitude was dominated by two events, one lasting 10 days in early May, the other lasting 20 days in June–July.

These estimates of persistence times are long compared with a minimum advection time scale ($L/U \sim 3$ days) for a water parcel moving at 80 cm/s to travel the length of a tongue 200 km long. The large currents and long persistence times suggest that the jets are continually fed by an upstream source or by strong recirculation.

It is also noteworthy that the time scale of 2–3 weeks is considerably shorter than the duration of the upwelling season. Maps of the upwelling-season means of surface temperature [*Kelly*, 1985] and nearshore (< 50 km) surface currents [*Davis*, 1985*b*] show only weak anomalies near Point Arena; this is further evidence that individual cold tongues and associated current jets do not persist through the entire upwelling season.

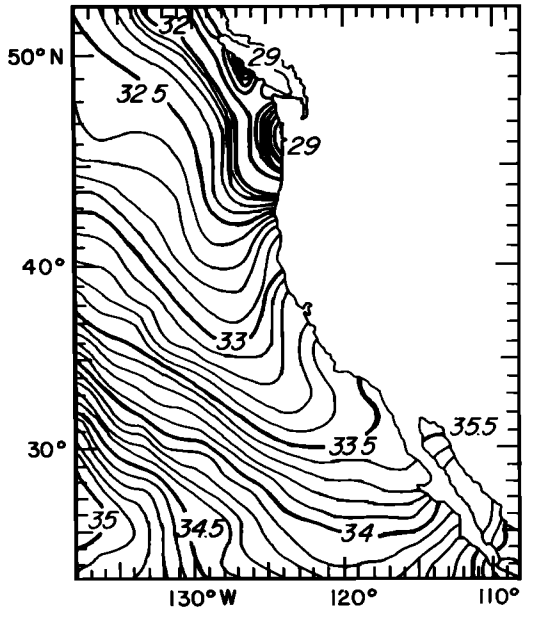

Fig. 8. Annual mean surface salinity in the California Current region [*Robinson*, 1976].

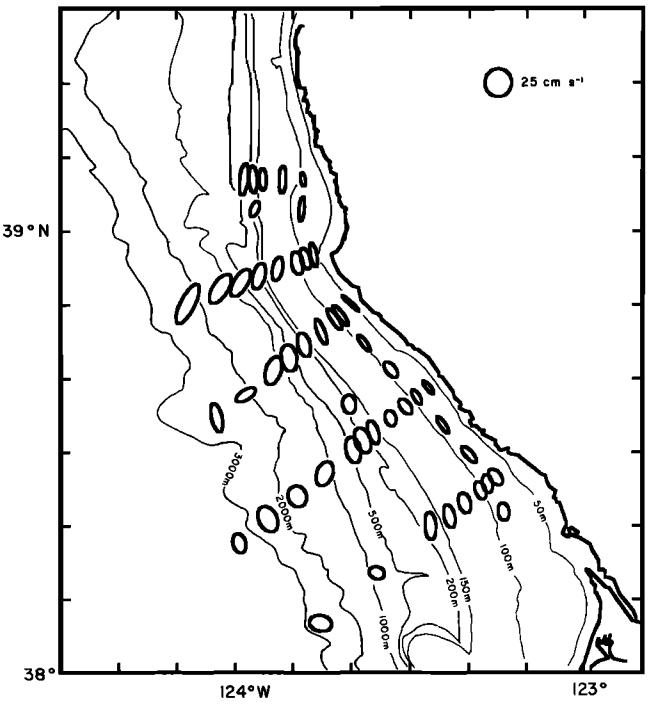

Fig. 9. Ellipses showing the orientation and magnitude of current variability over the continental shelf and slope near Point Arena. The semimajor and semiminor axes of each ellipse represent the principal axes of repeated DAL measurements made between April 26 and July 14, 1981, and between April 19 and July 27, 1982. Each ellipse represents at least eight observations [adapted from *Kosro*, 1985].

Mass Transport and the Coastal Jet

Integration of the DAL currents allowed us to directly calculate the mass transport through each of our sections over the depth range 15–125 m. Because currents were generally not negligible below 125 m, and because our transects often did not sample the full horizontal extent of the strong current features, such calculations can only set minimum bounds on the actual mass transport by the jets. Nevertheless, they provide an important clue to their source.

Measured upper ocean transports by the seaward jet averaged 1.5 sverdrups (1 sverdrup (Sv) = 10^6 m^3/s) over the uninterrupted DAL crossings in 1982; values ranged as high as 3.2 Sv in 1981 and 2.3 Sv in 1982. This much mass could not be supplied by a simple alongcoast concentration of the wind-driven offshore Ekman transport. A 1 dyn cm^{-2} (0.1 N m^{-2}) wind stress drives 10^{-3} Sv km^{-1} of offshore transport; it would require concentration of all the Ekman transport forced by 20-knot winds along ~1000 km of coast to provide the average of 1.5 Sv. Rather, in both years it appears that the offshore jet is downstream from and continuous with a strong jetlike alongshore flow (Figure 6). The peak of this alongshore flow lies at or beyond the shelf break in both years. Measured equatorward transports across the coastal sections, again limited to near-surface data and partial transects, ranged as high as 2.1 Sv in 1981 and 1.3 Sv in 1982; these are of the same order as the measured offshore transport in the seaward jet.

Equatorward "coastal jets" that flow parallel to the coast have been observed in most major coastal upwelling regions: off Oregon [*Huyer*, 1983], Peru [*Brink et al.*, 1983], northwest Africa [*Mittelstaedt*, 1983], and in the Benguela Current region [*Nelson and Hutchings*, 1983], with maximum equatorward currents occurring at the front between the dense recent-

ly upwelled waters and the warm, light oceanic surface waters. The alongshore extent of these coastal jets has not been established, since the direct evidence for them was obtained primarily from local experiments with an alongshore extent of about 50 km. *Freitag and Halpern* [1981], in one of the few detailed, large-scale hydrographic surveys off northern California, found upwelling along the entire coast between 43°N and 37°N in May 1977. Their maps of dynamic topography relative to 900 dbar show a continuous equatorward current over the slope between 43°N and 40°N. From Cape Mendocino south, however, the current field over the slope was found to be much more complex, with strong seaward and shoreward branches, and even northward surface flow between Cape Mendocino and Point Arena.

It is possible that the seaward jets represent an offshore deflection of the alongshore coastal jet. On the other hand, it is also possible that they are simply manifestations of a random field of eddies whose effects reach up onto the shelf, but which are spawned elsewhere. If the jets were found to recur at the same location along the coast, it would argue for local, rather than remote, formation.

Topographic Anchoring

During the upwelling seasons of 1981 and 1982, DAL measurements made repeatedly over the shelf and slope in the CODE region indicated that large fluctuations in the onshore/offshore component of the currents are recurrent features off Point Arena. Figure 9 shows the results of a principal axis analysis of DAL currents at locations that were occupied repeatedly (at least eight times) during CODE. Near the coast, current fluctuations are seen to be strongly polarized along the shelf bathymetry, as observed off Oregon [*Kundu and Allen*, 1976]. Farther from shore, the fluctuations continue to be aligned with the bottom topography but become less polarized until, in deep water, the fluctuations are approximately isotropic and the orientation of the principal axes becomes random. Offshore from Point Arena, however, the fluctuations remain strongly polarized, and the major axes turn offshore, distinctly across the local isobaths (Figure 9). These results, along with the EOF analysis of satellite-derived sea surface temperatures [*Kelly*, 1985], support the idea that cold tongues and cross-shore current jets occur preferentially at coastal capes and promontories.

CONCLUSIONS

In situ measurements obtained in July 1981 and July 1982 have revealed that the tongues or plumes of cold water observed in satellite images off the California coast were the surface manifestation of hydrographic anomalies that extended at least 100 m into the water column. The edge of the cold tongue separated surface waters with differing TS properties, and salinity appeared to be at least as important as temperature in determining surface density. The cold tongues were associated with seaward current features (jets or squirts) that flowed along the water mass boundary. The seaward jets were strong (directly measured currents reach 80 cm/s), highly sheared both vertically (occasionally exceeding 0.01 s^{-1}) and horizontally (observed range $-f/3$ to $+f$), and largely geostrophic. These jets had observed mass transports averaging more than 1.5 Sv and inferred time scales of 2–3 weeks. The seaward jets appeared to be continuous with and to have near-surface mass transports similar to alongshore current jets further north. Some evidence exists in the statistics of both the temperature and current fields to suggest that the cold tongues and current jets, while not steady features, were recurrent features in the fluctuations off Point Arena.

It should be noted that these observations represent samples from only two events, obtained in a single region during the same time of year. The degree to which the results presented here can be generalized to other seasons, other locations along the California coast, or other eastern boundary regions can be assessed only after completion of further studies, some of which are already in progress.

Acknowledgments. We wish to thank all those who made these surveys possible, especially Russ Davis and Lloyd Regier, who supported the DAL system and fostered its use in CODE; Kathie Kelly, who shared the results of her satellite images; Martin Olivera, who carried out the early analysis of the 1981 CTD data; Pierre Flament, who assisted in the analysis of the satellite images; and Rich Schramm and Jane Fleischbein for their part in collecting and processing the CTD data. Larry Armi provided the underway sampling system and the real time access to satellite IR images in July 1982, under funding by the Office of Naval Research. The observations and analysis presented here were funded by the National Science Foundation (grants OCE-8014943 and OCE-8410861 to Oregon State University and grant OCE-8410546 to Scripps Institution of Oceanography) and by the Office of Naval Research (contract N00014-80-C-0440 to Scripps Institution of Oceanography).

REFERENCES

Bernstein, R. L., L. C. Breaker, and R. Whritner, California Current eddy formation: Ship, air and satellite results, *Science*, *195*, 353–359, 1972.

Breaker, L. C., and R. P. Gilliland, A satellite sequence on upwelling along the California coast, in *Coastal Upwelling*, edited by F. A. Richards, AGU, Washington, D. C., 1981.

Brink, K. H., D. Halpern, A. Huyer, and R. L. Smith, The physical environment of the Peruvian upwelling system, *Progr. Oceanogr.*, *12*, 285–306, 1983.

CODE Group, Coastal Ocean Dynamics Experiment (CODE): A preliminary program description, *Eos Trans. AGU*, *64*, 538–540, 1983.

Davis, R. E., Drifter observations of coastal surface currents during CODE: The method and descriptive view, *J. Geophys. Res.*, *90*, 4741–4755, 1985*a*.

Davis, R. E., Drifter observations of coastal surface currents during CODE: The statistical and dynamical views, *J. Geophys. Res.*, *90*, 4756–4772, 1985*b*.

Flament, P., L. Armi, and L. Washburn, The evolving structure of an upwelling filament, *J. Geophys. Res.*, *90*, 11765–11778, 1985.

Freitag, H. P., and D. Halpern, Hydrographic observations off northern California during May 1977, *J. Geophys. Res.*, *86*, 4248–4252, 1981.

Gilbert, W. E., A. Huyer, and R. E. Schramm, Hydrographic data from the First Coastal Ocean Dynamics Experiment: R/V *Wecoma*, Leg 2, 10–14 April 1981, *Ref. 81-12*, 34 pp., Sch. of Oceanogr., Oreg. State Univ., Corvallis, 1981.

Huyer, A., Coastal upwelling in the California Current system, *Progr. Oceanogr.*, *12*, 259–284, 1983.

Huyer, A., J. Fleischbein, and R. Schramm, Hydrographic data from the second Coastal Ocean Dynamics Experiment: R/V *Wecoma*, Leg 9, 6–27 July 1982, *Ref. 84-7*, 130 pp., Sch. of Oceanogr., Oreg. State Univ., Corvallis, 1984.

Ikeda, M., and W. J. Emery, Satellite observations and modeling of meanders in the California Current system off Oregon and northern California, *J. Phys. Oceanogr.*, *14*, 1434–1450, 1984.

Kelly, K. A., Infrared satellite data from the first Coastal Ocean Dynamics Experiment, March–July 1981, *SIO Ref. 82-15*, 58 pp., Scripps Inst. of Oceanogr., La Jolla, Calif., 1982.

Kelly, K. A., The influence of winds and topography on the sea surface temperature patterns over the northern California slope, *J. Geophys. Res.*, *90*, 11783–11798, 1985.

Kosro, P. M., Shipboard acoustic current profiling during the Coastal Ocean Dynamics Experiment, Ph.D. thesis, *SIO Ref. 85-8*, 119 pp., Scripps Inst. of Oceanogr., La Jolla, Calif. 1985.

Kundu, P. K., and J. S. Allen, Some three-dimensional characteristics of low-frequency current fluctuations near the Oregon coast, *J. Phys. Oceanogr.*, *6*, 181–199, 1976.

Mittelstaedt, E., The upwelling area off northwest Africa—A description of phenomena related to coastal upwelling, *Progr. Oceanogr.*, *12*, 307–332, 1983.

Nelson, G., and L. Hutchings, The Benguela upwelling area, *Progr. Oceanogr.*, *12*, 333–356, 1983.

Olivera, M., W. E. Gilbert, J. Fleischbein, A. Huyer, and R. Schramm, Hydrographic data from the first Coastal Ocean Dynamics Experiment: R/V *Wecoma*, Leg 7, 1–14 July 1981, *Ref. 82-8*, 170 pp., Sch. of Oceanogr., Oreg. State Univ., Corvallis, 1982.

Olivera, R. M., A complex distribution of water masses and related circulation off northern California in July, 1981, Master's thesis, 53 pp., Sch. of Oceanogr., Oreg. State Univ., Corvallis, 1983.

Regier, L., Mesoscale current fields observed with a shipboard profiling acoustic current meter, *J. Phys. Oceanogr.*, *12*, 880–886, 1982.

Rienecker, M. M., C. N. K. Mooers, D. E. Hagan, and A. R. Robinson, A cool anomaly off northern California: An investigation using IR imagery and in situ data, *J. Geophys. Res.*, *90*, 4807–4818, 1985.

Robinson, M. K., Atlas of North Pacific Ocean monthly mean temperatures and mean salinities of the surface layer, *Ref. Publ. 2*, Nav. Oceanogr. Office, Washington, D. C., 1976.

Traganza, E. D., J. C. Conrad, and L. C. Breaker, Satellite observations of a cyclonic upwelling system and giant plume in the California Current, in *Coastal Upwelling*, edited by F. A. Richards, pp. 228–241, AGU, Washington, D. C., 1981.

A. Huyer and P. M. Kosro, College of Oceanography, Oregon State University, Corvallis, OR 97331.

(Received October 24, 1985;
accepted December 2, 1985.)